ICEUBI2015 University of Beira Interior Faculty of Engineering Covilhã | Portugal
December 2 3 4 International Conference on Engineering
Engineering for Society

Aerodynamic Performance of Aerofoils Obtained from a Geometric Offset Applied to a Given Initial Aerofoil

Diogo B. Sousa, David R. B. Melo, Pedro V. Gamboa
Department of Aerospace Sciences, Faculty of Engineering, University of Beira Interior, Covilhã, Portugal
diogo.bento.sousa@gmail.com, davidrbmelo@gmail.com, pgamboa@ubi.pt

Abstract

Many projects concerning morphing aircraft concepts where enhanced performance and increased energy efficiency are two of the main goals have been recently developed. Some of those concepts deal with wing span changes. In line with those, in a variable-span wing of the telescopic type, the cross-sections of the sliding panels, whether be two, three or more, must be made geometrically compatible among them. This requirement serves two purposes: to minimize the aerofoils geometric discontinuity which negatively affects wing drag and lift; and to provide a simple structural support between any two sliding panels. This paper describes the methodology employed to develop geometrically compatible aerofoils obtained from a constant geometric offset applied to a given initial aerofoil. This methodology is used to create inner offset aerofoils and outer offset aerofoils. The geometric and aerodynamic characteristics of the resulting offset aerofoils are compared with those of the original aerofoils. From the analysis of three different original aerofoils, strong trends on the geometric changes and on the aerodynamic characteristics of the resulting inner and outer offset aerofoils are observed. Ultimately, this study can help a telescopic wing designer decide whether an inner or an outer offset aerofoil is more appropriate for his/her design.

Keywords: aerofoil offset, aerofoil geometry, aerodynamic analysis, morphing technologies, variable-span wing, XFOIL

1. Introduction

Morphing wing technologies for flight regime adaptation have received great attention recently and may become important for aircraft's operations in near-optimal overall flight efficiency point. Advances in these technologies enable new design approaches and improvements in multi-task flexibility, by considering wing geometric transformations. A thorough review of morphing concepts that thrived to be functional in flight is presented by Barbarino [1] showing the huge effort of researchers to develop efficient and reliable morphing aircraft systems.

From an aerodynamics perspective, the overall shape of the wing (including cross-section) is the most important design aspect for an aircraft so that there is usually an ideal single configuration of the aircraft suitable for each specific type of mission [2]. Therefore a non-morphing aircraft is highly efficient in some design flight conditions while it becomes less suitable in others. Furthermore, morphing wing technologies contribute for efficient performance during distinct mission roles, or enable new multi-role missions that are not possible with a fixed geometry aircraft, as demonstrated by Tidwell et al [3].

Many projects have focused on aircraft morphing concepts with the ultimate goal of enhancing performance and increasing energy efficiency of aircraft [4]. As these technologies are still recent and lack adequate maturity, their progress is an iterative process between design and experiment. Also, a large number of projects have produced extensive work on aerodynamic shape optimization of aerofoils and multidisciplinary design optimization of wing systems [5-9]. Methods of aerofoil and wing morphing can include thickness and camber change [10], variable twist, variable chord, sweep change, and variable span [5]. Moreover, unmanned aerial vehicles (UAVs) have great potential for testing morphing technologies due to their flexibility, simple operation, low production and operation costs and the absence of direct risk to the crew. All in all, due to their characteristics, UAV concepts usually minimize the disadvantages and maximize the advantages of several research assignments.

The motivation behind the present work lies in the desire to improve a variable-span wing (VSW) design of the telescopic type previously developed at the Aerospace Sciences

Department of University of Beira Interior [8, 9, 11]. This new VSW design will make use of purposely optimized aerofoil sections and will also include aerofoil camber changes. The variable span capability allows the wing to be fully extended for take-off and landing, in a configuration of high lift where the lift-to-drag ratio is improved, and provide reduced take-off and landing distances. The fully extended span configuration is also suitable for low speed loiters. On the other hand, with the outboard panel retracted, while in cruise or at high speeds, the wing planform area and aspect ratio are reduced, decreasing parasite drag for improved range and cruise efficiency [11]. In this manner, the layout of the VSW concept is based on a hollow inboard fixed wing (IFW) that is fixed to the fuselage inside of which slides an outboard moving wing (OMW) slides actuated by an electromechanical mechanism.

The shape and size of the VSW is obtained through an in-house computational constrained aerodynamic shape optimization code, aimed at determining the wing mean chord and span values that minimize its drag for a specified mission profile. A detailed description of the aerodynamic optimization procedure is given by Albuquerque et al [12]. As inputs to this optimization procedure, two aerofoils' data points must be provided. For such task, it is mandatory to design two geometrically compatible aerofoils, with the chord length of the IFW larger than that of the OMW, in order for the outboard wing panel to slide inside the inboard wing panel. Accordingly, both IFW and OMW wing panels have the design constraint of keeping chord and aerofoil geometry constants along each panel's span, enabling proper fitting and support of the OMW.

Proper aerofoil design to ensure geometric compatibility and good aerodynamic performance is essential to guarantee improved overall variable-span wing performance over a conventional fixed wing. Thus, the main objective of this work is to develop aerofoils obtained from inward and outward geometric offsets applied to a given initial aerofoil to ensure geometric compatibility and to assess their resulting shape and aerodynamic characteristics compared with the original aerofoil. In the future the analysis methodology presented may help the designer decide whether inner offset or outer offset aerofoils are more suitable for a given application.

2. Offset Aerofoils

In a variable-span wing of the telescopic type, the cross-sections of the sliding panels, whether be two, three or more, must be made geometrically compatible among them. This requirement serves two purposes: to minimize the aerofoils geometric discontinuity which negatively affects wing drag and lift; and to provide a simple structural support between any two panels. As outlined in Mestrinho et al [8], a convenient way to match the IFW aerofoil to the OMW aerofoil of a two-panel telescopic wing is to create an aerofoil for the IFW from a positive (outer) offset of the aerofoil selected for the OMW so that the smallest possible discontinuity between wing sections is obtained. However, it is not clear weather this procedure is the most appropriate for any given general situation where maximum aerodynamic performance is mandatory. Therefore, the need to validate the decision of selecting a more adequate combination between keeping an original aerofoil for the OMW and the corresponding modified aerofoil with an outer offset for the IFW or, alternatively, setting the original aerofoil for the IFW, modifying it with an inner offset for the OMW, has emerged.

Due to the geometric modifications obtained by offsetting the original aerofoil shapes, small geometric conflicts or imperfections need to be corrected in the aerofoil regions near the leading edge (LE) and the trailing edge (TE). Different mathematical representations were applied in order to improve the geometry of the LE and TE regions of the offset aerofoils and attain good aerodynamic performance.

This work is thereby, divided into two parts. Firstly, two new aerofoils are mathematically created based on the modification of a given aerofoil selected for a specific application, with inner and outer offsets, where the size of the offset is usually selected based on structural considerations; and simultaneously, the LE and TE geometries are adjusted with some specified methods inserted in the main mathematical implementation. Secondly, a

comparison of the aerodynamic performance of those two modified aerofoils relative to their respective initial aerofoil is performed. The algorithm to create the offset aerofoils was implemented in a spreadsheet although it could also be implemented using any suitable programing language. The following information is required to build the offset aerofoils:

- Original aerofoil data points (unit chord);
- Aerofoil's chord length;
- Offset value;
- TE thickness (only applicable for the outer offset); and,
- The desired starting point for the aerofoil's LE (only applicable for the inner offset).

The output results are the inner and outer offsets of the original aerofoil, using different order polynomial interpolation for expanding the outer offset aerofoil's TE and different types of curves for rebuilding the inner offset aerofoil's LE.

3. Methodology

3.1. Offset Creation

The spreadsheet used to create the desired offset aerofoils is based on the original aerofoil data points. Each of the inner or outer offset aerofoil points are created using a normal vector, that has a predefined length (the offset) chosen by the user, which is perpendicular to the original aerofoil's surface at any given point.
Each normal vector that gives the position of the respective offset point is defined by inverting the slope of the respective vector tangent to the original aerofoil (computed by central finite differences in the present case). This operation gives the slope of the normal vector. Knowing the position of each point of the original aerofoil, the slope of the normal vector and the desired offset length (negative for the inner offset and positive for the outer offset), the offset aerofoil points' position can then be obtained from trigonometry.

3.2. Outer Offset and Trailing Edge Extension

In the case of the outer offset, the critical situation lies in the creation of a TE. The TE of the outer offset has to be extended so that the desired gap thickness is respected. Polynomial functions were used for this purpose, using at least two points at the TE of the offset modified aerofoil.
The original aerofoil is unit chord and thus the offset value must be divided by the chord length before the desired offset geometry is calculated. The TE is created using different polynomial interpolations using the last points of the upper and lower surfaces of the aerofoil (starting from around 95% to 100% of the offset aerofoil's chord). The polynomial interpolations can be of different order (typically, first, second and third order). Figure 1 shows one example where a second order polynomial was applied to the TE.

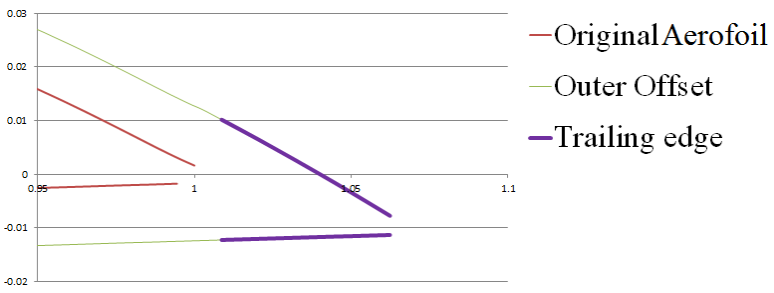

Figure 1 – TE extension at the outer offset aerofoil.

3.3. Inner Offset and Leading Edge

As illustrated in Figure 2, the inner offset of an aerofoil creates a sharp LE due to the intersection of the normal offset of the upper and lower surfaces of the aerofoil. This critical situation imposes the creation of a new round LE. As mentioned previously, a distance from the original aerofoil LE must be provided indicating the new offset aerofoil LE position. Different methodologies were attempted to create the desired smooth LE, such as a parabolic function, a double-parabolic function or double-ellipse function. The methodology that provided the best new LE was the double-ellipse function. This methodology consisted on using two ellipse functions, one for the upper surface and another for the lower surface of the aerofoil, which must be tangent to the offset modified aerofoil and pass through the specified shared new LE point. An example of this method is illustrated in Figure 3.

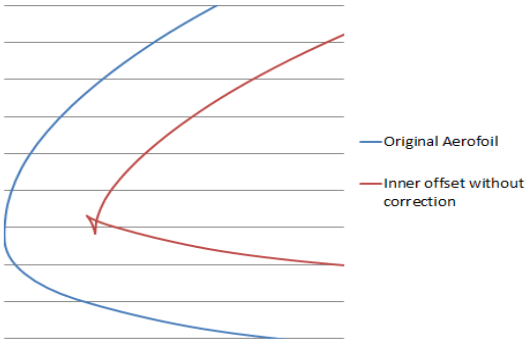

Figure 2 – LE curve at the inner offset aerofoil.

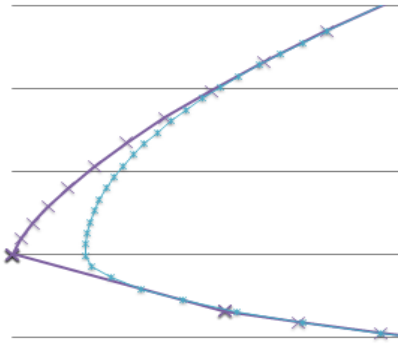

Figure 3 – Double-elliptical function LE curve at the inner offset aerofoil.

With this ellipse definition, three boundary conditions can be imposed, i.e., each ellipse function should:

- Pass through the user's defined new LE point of the offset modified aerofoil;
- Confirm the tangent condition to the offset modified aerofoil; and,
- Pass perpendicularly through the same new LE point.

The z coordinate of each point of the new round LE is fixed to create a constant mesh size (in the z direction) between the upper and lower limits of the new round LE, so that the only variable to be defined is then the x coordinates of the points.
The ellipse function is as follows,

$$\frac{(x-x_0)^2}{a^2}+\frac{(z-z_0)^2}{b^2}=1 \Rightarrow x=\mathrm{x}_0+\frac{a}{b}\sqrt{b^2-z^2} \quad (1)$$

where x_0+a and $z_0=0$ are the ellipse's centre point coordinates, x_{LE} is the x coordinate of the new LE point, and a and b are half the width and height of the ellipse, respectively. It is worth pointing out that all dimensions here are relative to the aerofoil's chord length.
In order to guarantee the tangency of the new LE curve with the aerofoil surface, the derivative of the function with respect to z is required as follows

$$\frac{dx}{dz}=\frac{\mathrm{a\ z}}{b\sqrt{b^2-z^2}} \quad (2)$$

Solving Equations (1) and (2), for the upper and lower sides of the new LE, the only unknown variables *a* and *b*, can be computed. Consequently, both ellipse functions defining the new LE can be created.

3.4. Aerodynamic Analysis

The 2-dimentional (2D) aerodynamic coefficients as functions of the angle of attack, α, and Reynolds number, *Re*, were obtained using XFOIL [13]. In XFOIL, the steady Euler equations in integral form are used to represent the inviscid flow, and a compressible lag-dissipation integral method is used to represent the boundary layers and wake. The entire viscous solution (boundary layers and wake) is strongly interacted with the incompressible potential flow via the surface transpiration model, which permits proper calculation of limited separation regions. Thus, data for the aerofoils lift coefficient, C_l, curves, aerofoils parasite drag coefficient, C_d, curves, including the non-linear regime, were obtained from this aerofoil aerodynamic analysis program. The aerofoil lift-to-drag versus C_l curves were also obtained.

4. Case Studies and Results

In the study of a new high performing two-panel telescopic wing, three aerofoils are initially considered as suitable candidates: modified MH115, modified SG6042 and UBI-O3-012. These aerofoils are low speed aerofoils with a good compromise between maximum lift coefficient, C_{lmax}, maximum lift-to-drag ratio, $(L/D)_{max}$, and low drag coefficient, C_d, in the speed range from about 13 m/s to 30 m/s. The maximum thickness ratio, $(t/c)_{max}$, of the modified MH115 is 11.3% whilst that of the other two aerofoils is 10%. Moreover, the concept applied to this study was based on the characteristics and flight conditions of a wing with a 280 mm mean chord and a 3 mm offset for the inner and outer modified aerofoils and, also, an aerodynamic analysis condition of constant $Re.C_l^{1/2}$ = 325,000.

The modified MH115 and modified SG6042 aerofoils are MH115 and SG6042 aerofoils, respectively, with their TE cut-off so that their thicknesses are 1 mm with the chord length mentioned above and are referred to as MH115 and SG6042 below. The MH115 aerofoil exhibits the highest camber, a C_{lmax} greater than 1.6 and has its $(L/D)_{max}$ of 107 for a C_l of around 1.2. The SG6042 aerofoil exhibits a C_{lmax} just over 1.5 and has its $(L/D)_{max}$ of 110 for a C_l of around 0.9. The UBI-O3-012 aerofoil was developed in house through an optimization procedure applied to the SG6042 aerofoil to increase its C_{lmax} and reduce its drag coefficient, C_d, over a wider range of C_l values. This aerofoil exhibits a C_{lmax} just under 1.6 and has its $(L/D)_{max}$ of 112 for a C_l of around 0.9.

The methodology described previously was applied, entering the original/non-modified aerofoil coordinates and input data defined by the user. Novel aerofoils were created with the outer and inner offsets, as well as the determination of the most adequate LE and TE representations. It was observed that the elliptical LE for the inner offset aerofoils and the second order polynomial TE for the outer offsets produced the best aerodynamic performance.

Figure 4 shows the aerofoil geometries. Using the original aerofoil with unit chord (represented in black), the inner offset aerofoil was obtained (represented in green) together with the outer offset aerofoil (represented in red). On the left hand column the aerofoils are represented to scale relative to the original aerofoil whilst on the right hand column they are all illustrated with unit chord for better geometry comparison. For all three original aerofoils, the offsets present identical trends. The inner offset produces an aerofoil with reduced maximum camber and maximum thickness ratio, whose positions move slightly aft, and with decreased incidence. On the other hand, the outer offset produces an aerofoil with increased maximum camber and maximum thickness ratio, whose positions move slightly forward, and with increased incidence. Other important aspects of the aerofoil geometry are the TE thickness and TE angle. It is observed that, the smaller the original TE angle, the greater will be the variation in chord of the offset aerofoils provided the curvature of the upper and lower surfaces at the TE are not highly different as is the case with the UBI-O3-012 aerofoil. In general, and from a structural point of view, thicker aerofoils are preferred for the inboard panels due to the higher structural depth, and higher TE angles result in stiffer offset TE's and smaller variations in chord lengths.

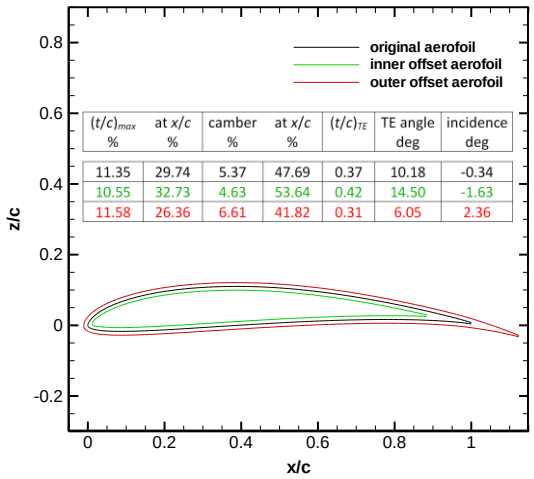

$(t/c)_{max}$ %	at x/c %	camber %	at x/c %	$(t/c)_{TE}$	TE angle deg	incidence deg
11.35	29.74	5.37	47.69	0.37	10.18	-0.34
10.55	32.73	4.63	53.64	0.42	14.50	-1.63
11.58	26.36	6.61	41.82	0.31	6.05	2.36

(a) MH115 and offset aerofoils.

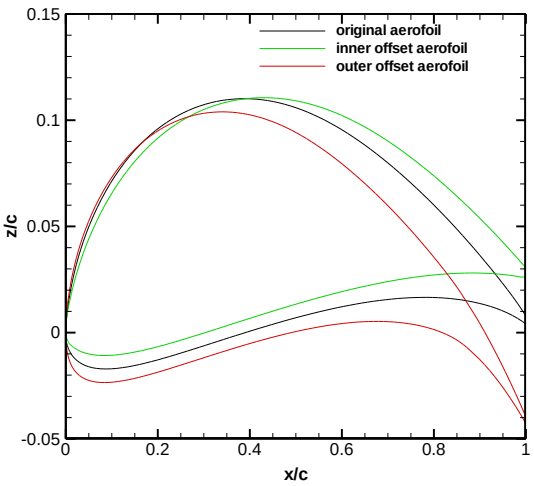

(b) MH115 and *unit chord* offset aerofoils.

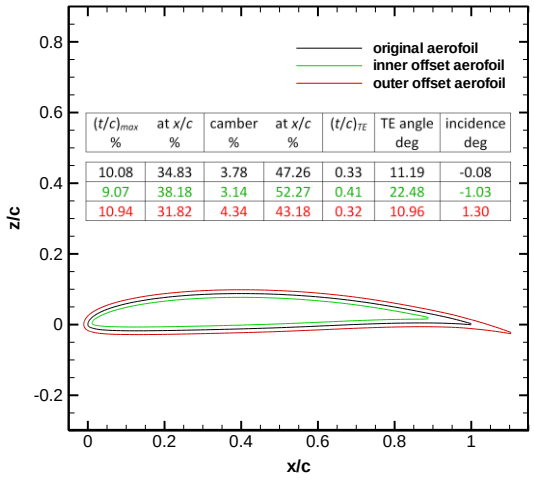

$(t/c)_{max}$ %	at x/c %	camber %	at x/c %	$(t/c)_{TE}$	TE angle deg	incidence deg
10.08	34.83	3.78	47.26	0.33	11.19	-0.08
9.07	38.18	3.14	52.27	0.41	22.48	-1.03
10.94	31.82	4.34	43.18	0.32	10.96	1.30

(c) SG6042 and offset aerofoils.

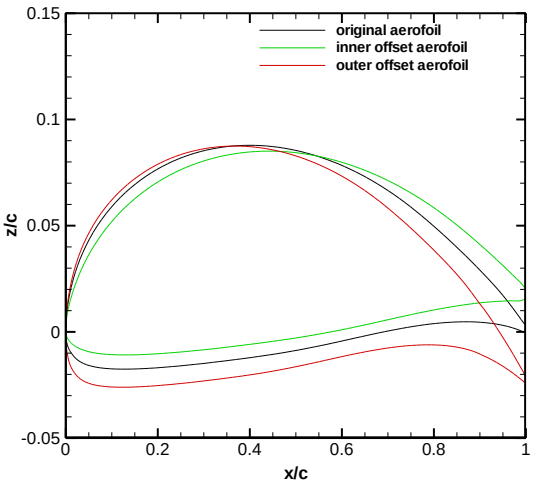

(d) SG6042 and *unit chord* offset aerofoils.

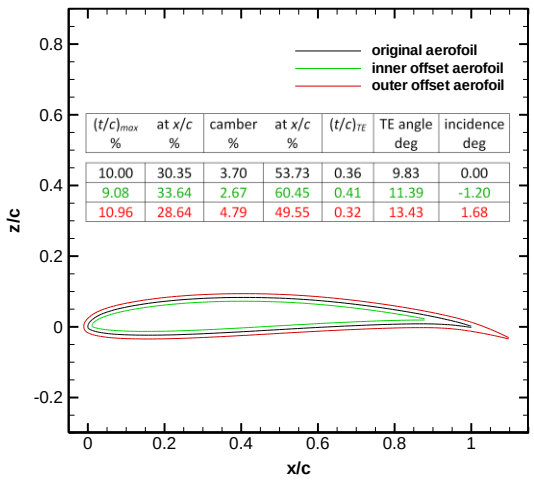

$(t/c)_{max}$ %	at x/c %	camber %	at x/c %	$(t/c)_{TE}$	TE angle deg	incidence deg
10.00	30.35	3.70	53.73	0.36	9.83	0.00
9.08	33.64	2.67	60.45	0.41	11.39	-1.20
10.96	28.64	4.79	49.55	0.32	13.43	1.68

(e) UBI-O3-012 and offset aerofoils.

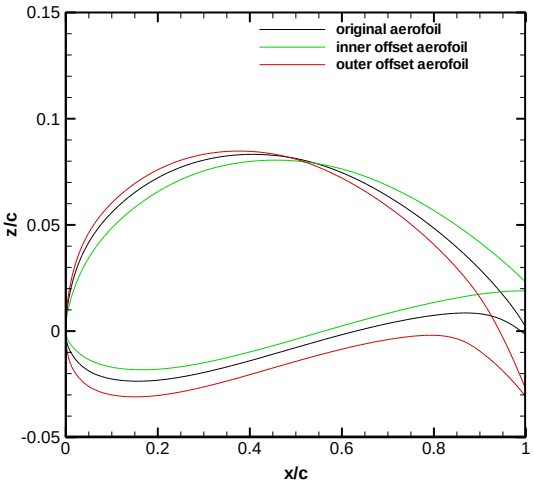

(f) UBI-O3-012 and *unit chord* offset aerofoils.

Figure 4 – Original aerofoils and aerofoils obtained by inner and outer offsets: on the left hand column the aerofoils are shown to scale; and on the right hand column the aerofoils are non-dimensionalized to unit chord.

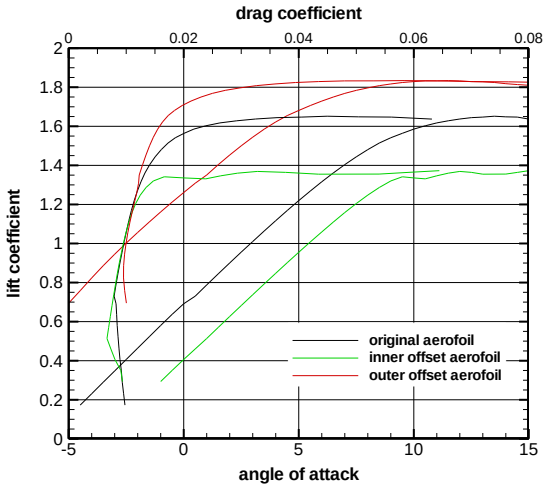

(a) MH115 lift curves and drag polars.

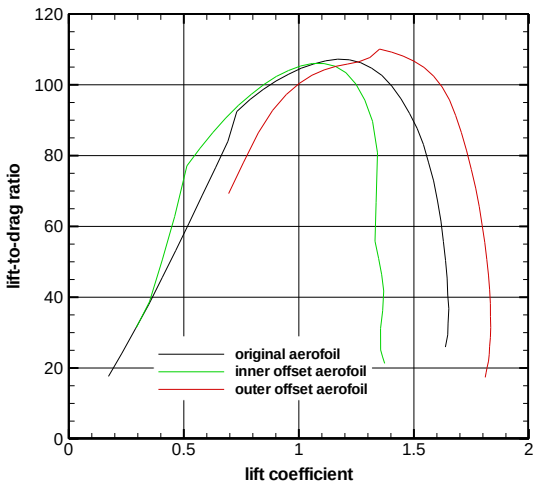

(b) MH115 lift-to-drag ratio curves.

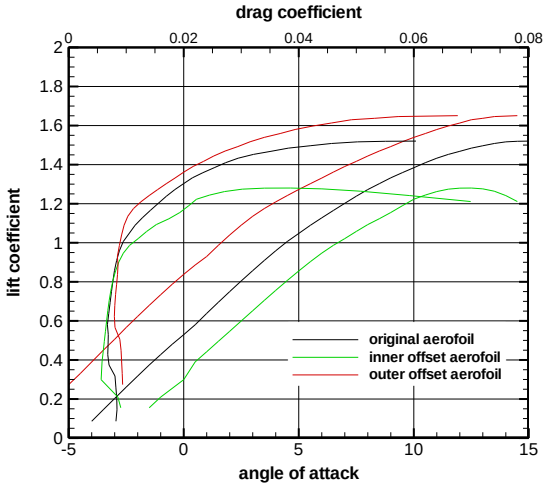

(c) SG6042 lift curves and drag polars.

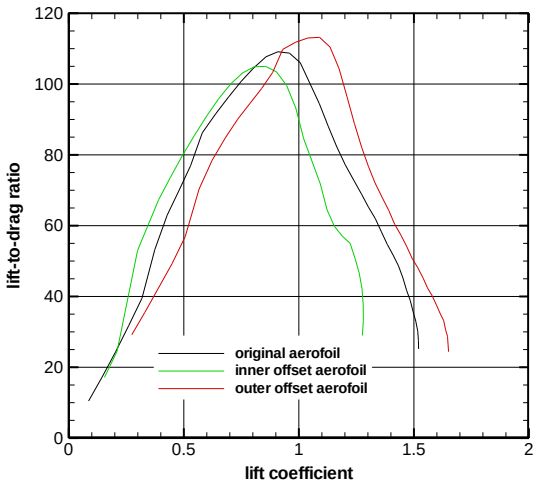

(d) SG6042 lift-to-drag ratio curves.

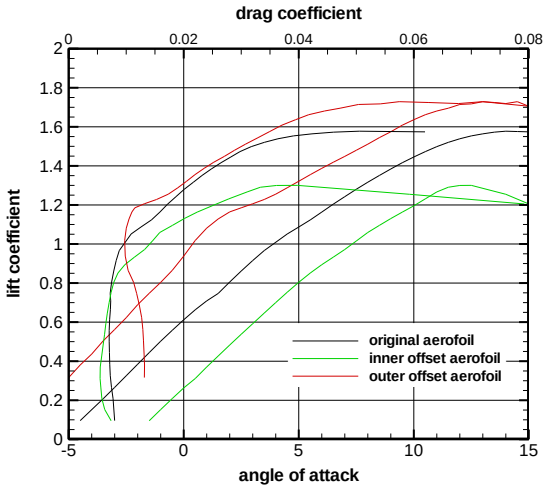

(e) UBI-O3-012 lift curves and drag polars.

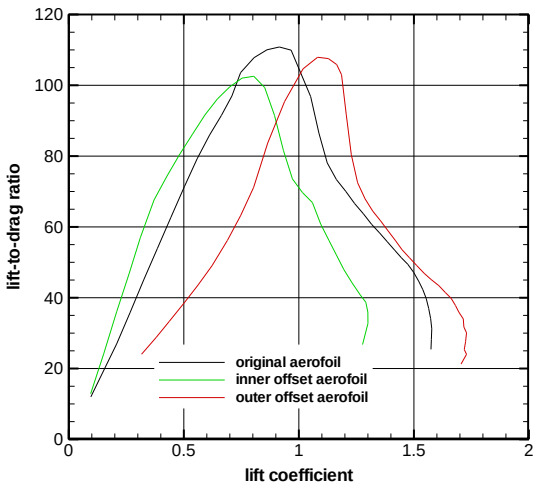

(f) UBI-O3-012 lift-to-drag ratio curves.

Figure 5 – Aerodynamic data obtained for the original aerofoils and the aerofoils obtained by inner and outer offsets at $Re.C_l^{1/2}$ = 325,000: on the left hand column the lift curves and drag polars are shown; and on the right hand column the lift-to-drag ratio curves are shown.

Those geometric modifications also have strong effects on the aerodynamic characteristics of the resulting aerofoils and must be investigated. Figure 5 illustrates the main aerodynamic characteristics of the studied aerofoils at $Re.C_l^{1/2}$ = 325,000. On the left hand column the lift curves (C_l x α curves) and the drag polars (C_l x C_d curves) are shown whilst on the right hand column the lift-to-drag ratio curves (L/D x C_l curves) are represented.
From the lift curves, it is observed that the outer offset aerofoil produces an increase in C_{lmax} and in the zero-angle of attack lift coefficient, C_{l0}. Its drag polar is moved to larger C_l values, resulting that $(L/D)_{max}$ occurs at a higher C_l value, and the minimum C_d value is slightly increased. Not shown in Figure 6, but also an important result, the pitching moment coefficient becomes more intense in the outer offset aerofoil. The opposite is true for the inner offset aerofoil. These results were expected since the outer offset aerofoils' mean camber and incidence were positively incremented and the inner offset aerofoils' mean camber and incidence were decremented. It is interesting to point out that $(L/D)_{max}$ increases with the outer offset and decreases with the inner offset for the MH115 and SG6042 aerofoils. The same is not seen with the UBI-O3-012 aerofoil, where $(L/D)_{max}$ occurs for the original aerofoil and not for the outer offset aerofoil, but its lowest value is still exhibited by the inner offset aerofoil. The reduced $(L/D)_{max}$ in the outer UBI-O3-012 offset aerofoil may be explained by the narrower laminar flow region observed in the drag polar curve, indicating that the laminar boundary layer in this case cannot extend so further aft at higher C_l values as with the other two aerofoils. Stall characteristics do not seem to be affected since the shape of the lift curves in the stall region do not present any significant differences among them.

5. Conclusions

A methodology for developing offset aerofoils given any existing aerofoil, including corrections for the leading edge and trailing edge geometries of the resulting aerofoils, was presented. The analysis of the offset aerofoils obtained from three initial known aerofoils enabled a better understanding of the geometric changes suffered by the offset aerofoils and the effect on their aerodynamic characteristics.
From the three aerofoils studied the following trends could be observed. In terms of the geometric characteristics:

- The inner offset aerofoils have: reduced maximum camber at a further aft chord position; reduced $(t/c)_{max}$ at a further aft chord position; decreased incidence;
- The outer offset aerofoils have: increased maximum camber at a further fore chord position; increased $(t/c)_{max}$ at a further fore chord position; increased incidence.
- The smaller the trailing edge angle of the original aerofoil, the shorter and the longer will the inner and the outer aerofoils, respectively, be.

The above geometric characteristics produce the following aerodynamic properties trends:

- The inner offset aerofoils have: reduced C_{lmax}; reduced C_{l0}; reduced $(L/D)_{max}$ and corresponding C_l; less intense pitching moment coefficient; reduced minimum C_d and corresponding C_l;
- The outer offset aerofoils have: increased C_{lmax}; increased C_{l0}; increased $(L/D)_{max}$ and corresponding C_l, provided the laminar boundary layer still extends over a long distance on the upper surface; more intense pitching moment coefficient; increased minimum C_d and corresponding C_l.

The present study was not exhaustive but gave some hints on the geometry and performance trends expected from the development of offset aerofoil designs intended to be applied to telescopic wings. Specific design situations must be analysed to select and/or develop an adequate set of aerofoils.

Future work regarding the effects on employing an offset at a given aerofoil should focus on studying these same effects on different families of aerofoils (e.g. highly cambered aerofoils) and also exploring a larger range of Reynolds numbers. The outcome of these studies will help design a set of compatible aerofoils suitable for aircraft employing telescopic wing concepts.

Acknowledgements

This work has been partially funded by the European Community's Seventh Framework Programme (FP7) under the Grant Agreement 314139. The CHANGE project (Combined morphing assessment software using flight envelope data and mission based morphing prototype wing development) is a Level 1 project funded under the topic AAT.2012.1.1-2. involving 9 partners. The project started on August 1st 2012.

References

[1] Barbarino, S.; Bilgen, O.; Ajaj, R.M.; Friswell, M.I.; Inman, D. J.: "A review of Morphing Aircraft", *Journal of Intelligent Material Systems and Structures*, Vol. 22 nº9 (2011), DOI 10.1177/1045389X11414084, pp. 823-877.

[2] Amador, M.B.; Kulkarni, V.: "Morphing Wing Design for UAVs: A proposed Concept", BSc Thesis, Department of Mechanical and Industrial Engineering, University of Toronto, 2009.

[3] Tidwell, Z.; Joshi, S.; Crossley, W.; Ramakrishnan, S.: "Comparison of Morphing Wing Strategies Based Upon Aircraft Performance Impacts", AIAA Paper 2004-1722, *45th AIAA/ASME/ASCE/AHS/ASC Structures, Structural Dynamics and Materials Conference*, Palm Springs, California, 19-22 April, 2004.

[4] Flanagan, J.S.; Strutzenberg, R.C.; Myers, R.B.; Rodrian, J.E.: "Development and Flight Testing of a Morphing Aircraft, the NextGen MFX-1", AIAA Paper 2007-1707, *48th AIAA/ASME/ASCE/AHS/ASC Structures, Structural Dynamics and Materials Conference*, Honolulu, Hawaii, 23-26 April, 2007.

[5] Neal, D.; Good, M.; Johnston, C.; Robertsha, H.; Mason, W.; Inman, D.: "Design and Wind-Tunnel Analysis of a Fully Adaptative Aircraft Configuration", AIAA Paper 2004-1727, *45th AIAA/ASME/ASCE/AHS/ASC Structures, Structural Dynamics and Materials Conference*, Palm Springs, California, 19-22 April, 2004.

[6] Secanell, M.; Suleman, A.; Gamboa, P.: "Design of a Morphing Aerofoil Using Aerodynamic Shape Optimization", *AIAA Journal*, Vol. 44 nº 7 (2006), pp. 1550-1562.

[7] Marques, M.; Gamboa, P.; Andrade, E.: "Design of a Variable Camber Flap for Minimum Drag and Improved Energy Efficiency", *50th AIAA/ASME/ASCE/AHS/ASC Structures, Structural Dynamics and Materials Conference*, Palm Springs, California, 4-7 May, 2009.

[8] Mestrinho, J.; Gamboa, P.; Santos, P.: "Design Optimization of a Variable-Span Morphing Wing for a Small UAV", AIAA Paper 2011-2025, *52th AIAA/ASME/ASCE/AHS/ASC Structures, Structural Dynamics and Materials Conference*, Denver, Colorado, 4-7 April, 2011.

[9] Felício, J.; Santos, P.; Gamboa, P.; Silvestre, M.: "Evaluation of a Variable-Span Morphing Wing for a Small UAV", AIAA Paper 2011-2074, *52th AIAA/ASME/ASCE/AHS/ASC Structures, Structural Dynamics and Materials Conference*, Denver, Colorado, 4-7 April, 2011.

[10] Gamboa, P.; Vale, J.; Lau, F.; Suleman, A.: "Optimization of a Morphing Wing Based on Coupled Aerodynamic and Structural Constraints", *AIAA Journal*, Vol. 47 nº 9, September 2009, pp. 2087-2104.

[11] Santos, P.; Sousa, J.; Gamboa, P.: "Variable-span wing development for improved flight performance", *Journal of Intelligent Material Systems and Structures*, 31 July 2015 (DOI:10.1177/1045389X15595296).

[12] Albuquerque, P.F.; Gamboa, P.V.; Silvestre, M.A.: "Multidisciplinary and Multilevel Aircraft Design Methodology using Enhanced Collaborative Optimization", *16th AIAA/ISSMO Multidisciplinary Analysis and Optimization Conference*, Dallas, Texas, 22-26 June 2015.

[13] Drela, M. *XFOIL 6.94 User Guide*. Technical Report., Massachusetts Institute of Technology & Astro Harold Youngren Aerocraft, Inc., USA, 10th of December 2001.